Structural Engineering and Mechanics, *Vol. 62, No. 6 (2017) 759-769*
DOI: https://doi.org/10.12989/sem.2017.62.6.759

On triply coupled vibration of eccentrically loaded thin-walled beam using dynamic stiffness matrix method

Elham Ghandi* and Babak Shiri[a]

Faculty of Technical and Engineering, University of Mohaghegh Ardabili, Ardabil, Iran

(Received August 11, 2016, Revised May 3, 2017, Accepted May 4, 2017)

Abstract. The effect of central axial load on natural frequencies of various thin-walled beams, are investigated by some researchers using different methods such as finite element, transfer matrix and dynamic stiffness matrix methods. However, there are situations that the load will be off centre. This type of loading is called eccentric load. The effect of the eccentricity of axial load on the natural frequencies of asymmetric thin-walled beams is a subject that has not been investigated so far. In this paper, the mentioned effect is studied using exact dynamic stiffness matrix method. Flexure and torsion of the aforesaid thin-walled beam is based on the Bernoulli-Euler and Vlasov theories, respectively. Therefore, the intended thin-walled beam has flexural rigidity, saint-venant torsional rigidity and warping rigidity. In this paper, the Hamilton's principle is used for deriving governing partial differential equations of motion and force boundary conditions. Throughout the process, the uniform distribution of mass in the member is accounted for exactly and thus necessitates the solution of a transcendental eigenvalue problem. This is accomplished using the Wittrick-Williams algorithm. Finally, in order to verify the accuracy of the presented theory, the numerical solutions are given and compared with the results that are available in the literature and finite element solutions using ABAQUS software.

Keywords: thin-walled beam; exact dynamic stiffness matrix; eccentric axial load; Wittrick-Williams algorithm; triply coupled vibration

1. Introduction

Thin-walled beams are basic structural elements that have found widespread use in most branches of structural engineering. In these beams, because of specific geometry characteristics, centroid and shear centre of typical cross-sections are not coincident (except symmetric sections). Therefore, the bending and torsional vibration modes of a thin-walled beam with mono-symmetric and asymmetric cross-sections will be coupled. Since thin-walled beams with coupled bending- torsional motion, have many practical applications, many efforts is done for solving vibration and buckling problems of them (Jun *et al.* 2004, Eken and Kaya 2015, Chen *et al.* 2016, Chen and Hsiao 2007, Sheikh *et al.* 2015 and Kim 2009). Finite element method, transfer matrix method and exact dynamic stiffness method are some methods that were used to solve vibration problems of mentioned beams.

Exact dynamic stiffness matrix method (EDSM) is a powerful means of solving vibration problems in structural engineering, particularly when higher natural frequencies and better accuracy are required (Banerjee 1997). The use of EDSM in vibration analysis of beams has certain advantages over the conventional finite element method. This is because, in the finite element method, the stiffness parameters of an individual element are derived from the assumed shape functions and so are not 'exact', whereas the properties obtained from EDSM are based on the closed form analytical solution of the differential equation of the element and hence are justifiably called 'exact'. Many researchers have used EDSM method in solving coupled bending-torsional vibration problems of beams. Banerjee (1989) derived explicit expressions for elements of dynamic stiffness matrix of a mono-symmetric Bernoulli-Euler beam. In next one, Banerjee (1991) wrote a FORTRAN subroutine for calculating the EDSM of coupled vibration of mentioned beam of former research. Banerjee and Williams (1992) derived analytical expressions for the elements of the dynamic stiffness matrix governing the coupled bending-torsional motion of a uniform Timoshenko beam. Banerjee *et al*. (1996) formulated an exact dynamic stiffness matrix for a Bernoulli-Euler thin-walled beam including the effects of warping torsion. Eslimy-Isfahany *et al*. (1996) investigated the response of a mono-symmetric beam coupled in bending and torsion to deterministic and random loads by using the EDSM and normal mode methods. Rafezy and Howson (2007) developed an exact dynamic stiffness matrix for the coupled flexural -torsional motion of a three dimensional bi-material beam of doubly asymmetric cross-section. Ghandi *et al*. (2012) extended Rafezy and Howson's work (2007) by replacing the Euler-Bernoulli theory with Timoshenko theory when modeling the beam's thin-walled outer layer. The papers mentioned so far do not allow for the effect of a static axial load in the member. Coupled vibration of beams under axial loading has been of practical interest in recent years. The additional

*Corresponding author, Assistant Professor
E-mail: Ghandi@uma.ac.ir
[a]Master of structural Engineering

http://www.techno-press.com/journals/sem&subpage=7 ISSN: 1225-4568 (Print), 1598-6217 (Online)

effect of axial load was considered by Banerjee and Fisher (1992), who derived analytical expressions for the coupled bending-torsional dynamic stiffness matrix based on Euler-Bernuolli theory. This was later extended by Banerjee and Williams (1994) to cover Timoshenko theory. Eslimy-Isfahany and Banerjee (1996) predicted the dynamic response of an axially loaded bending-torsional coupled beam to deterministic and random loads. Shirmohammadzade *et al*. (2011) used Bernoulli-Euler beam theory to develop an exact dynamic stiffness matrix for the flexural-torsional coupled motion of a three-dimensional, axially loaded, thin-walled beam of doubly asymmetric cross-section. Ghandi *et al*. (2015) developed the dynamic stiffness matrix of an axially loaded elastically supported uniform bi-material beam with doubly asymmetric cross-section and subsequently used to investigate it's free vibration characteristics. In all studies mentioned above, the axial load is applied in centroid. However, there are situations that the load will be off center and cause a bending in the member in addition to the tension or compression. This type of loading is called eccentric load. Such an eccentric load can be replaced by an equivalent axial load that is on the neutral axis and bending moment. In this paper the effect of an eccentric axial load on the coupled vibration of asymmetric thin-walled beams is studied using exact dynamic stiffness matrix method. Bernoulli-Euler and Vlasov theories are used to modeling the flexure and torsion of the aforesaid thin-walled beam, respectively.

2. Theory

The following basic assumptions are adopted in order to investigate the coupled vibration of eccentrically axially loaded asymmetric thin-walled beam:

1. All displacements and strains are small so that the theory of linear elasticity applies.
2. The beam is made of homogeneous and isotropic materials, so mass center and center of geometry of cross-section are coincident.
3. The thin-walled beam is prismatic.
4. The cross-section is rigid with respect to in-plane deformation except for warping deformation.

2.1 Governing differential equations

The first step towards developing the dynamic stiffness matrix of a structural element is to derive its governing differential equations of motion in free vibration. The structural model of an asymmetric prismatic thin-walled beam is shown in Fig. 1. The shear centre (O) and mass centre (C) of the beam are not coincident and are separated by distances x_c and y_c. The origin of xyz coordinate system is O and the origin of rsq coordinate system is C. The z-axis is assumed to coincide with the flexure axis and the q-axis is assumed to coincide with the mass axis. A constant eccentric axial load P is assumed to act through the arbitrary point (N) of the cross-section of the thin-walled beam. The eccentricities of P relative to centroid are e_r and e_s.

During vibration, the displacement of the shear and mass centers at any time t in the $x-y$ plane can be determined as the result of a pure translation followed by a pure rotation about the shear centre O. The flexural translation in the x and y directions and torsional rotation about the z-axis are represented by $u(z,t)$, $v(z,t)$ and $\varphi(z, t)$, respectively. The resulting translations (u_c, v_c) of the mass centre in the x and y directions, respectively, are

$$u_c(z,t) = u(z,t) - y_c\varphi(z,t) \tag{1a}$$

$$v_c(z,t) = v(z,t) + x_c\varphi(z,t) \tag{1b}$$

The governing equations of motion and the boundary conditions can be derived using Hamilton's principle

$$\int_{t_1}^{t_2} \delta(T-V)dt = 0 \quad (\delta u(z,t) = \delta v(z,t) = \delta\varphi(z,t) = 0 \quad at \quad t = t_1, \ t_2) \tag{2}$$

where δT and δV denote the variations of the kinetic and potential energies.

The kinetic energy T of the beam is given by

$$T = \frac{1}{2}\int_0^L m\left[(\dot{u}_c(z,t))^2 + (\dot{v}_c(z,t))^2 + r_{mc}^2(\dot{\varphi}(z,t))^2\right]dz \tag{3}$$

in which m is the mass per unit length and r_{mc} is the polar radius of gyration of the cross-section about mass axis

$$T = \frac{1}{2}\int_0^L m[((\dot{u}(z,t))^2 - 2y_c\dot{u}(z,t)\dot{\varphi}(z,t)) + ((\dot{v}(z,t))^2 + 2x_c\dot{v}(z,t)\dot{\varphi}(z,t)) + r_m^2(\dot{\varphi}(z,t))^2]dz \tag{4}$$

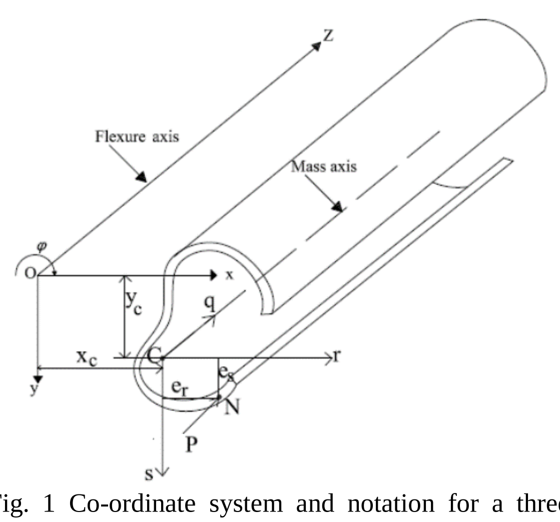

Fig. 1 Co-ordinate system and notation for a three-dimensional thin-walled axially loaded beam of length L that has a doubly asymmetric cross-section

where $r_m^2 = x_c^2 + y_c^2 + r_{mc}^2$ is the polar radius of gyration of the cross-section about flexure axis.

The total potential energy of the beam is expressed as follows

$$V = V_{\text{int}} - V_{ext} \tag{5}$$

in which V_{int} is the strain energy stored in the member and V_{ext} is the potential energy of the external loads.

The strain energy consists of four parts, the energies due to bending in the $x-z$ and $y-z$ planes, the energy of the Saint-Venant shear stresses and the energy of longitudinal stresses associated with warping torsion. Thus

$$V_{\text{int}} = \frac{1}{2}\int_0^L \left[EI_x \left(\frac{\partial^2 u(z,t)}{\partial z^2} \right)^2 + EI_y \left(\frac{\partial^2 v(z,t)}{\partial z^2} \right)^2 + G_t J_t \left(\frac{\partial \varphi(z,t)}{\partial z} \right)^2 + EI_w \left(\frac{\partial^2 \varphi(z,t)}{\partial z^2} \right)^2 \right] \tag{6}$$

where EI_x and EI_y are the flexural rigidity of the beam in the $x-z$ and $y-z$ planes, respectively. G_tJ_t and EI_w are the Saint-Venant and warping torsion rigidity, respectively.

The only external force applied to the cross-section is an eccentric axial load (P). So to achieve V_{ext}, the potential energy of the axial load should be calculated. The mentioned eccentric axial load can be considered as a combination of a central axial load and two bending moments in principal planes. Then the normal stress at any point of beam is given by the equation

$$\sigma = \frac{P}{A} + \frac{M_r . r}{I_r} + \frac{M_s . s}{I_s} \tag{7}$$

where $I_r = \int_A r^2 dA$ and $I_s = \int_A s^2 dA$ are the moment of inertia, A is the area of cross-section, M_r and M_s are the bending moments in $r-q$ and $s-q$ plans, respectively. These moments are defined by the equations

$$M_r = P.e_r \tag{8a}$$

$$M_s = P.e_s \tag{8b}$$

The potential energy of the external axial load is equal to the product of the load and the distance it moves as the member deforms. Fig. 2 shows a longitudinal fiber whose ends approach one another by an amount Δ when the fiber bends. The distance Δ is equal to the difference between the arc length b and the chord length L of the fiber. If the cross-sectional area of the fiber is dA, then the potential energy of the load acting on the fiber is $\Delta\sigma dA$.

The total potential energy for the entire member is obtained by integrating over the cross-sectional area. Thus

$$V_{ext} = \int_A \Delta\sigma dA \tag{9}$$

The Δ parameter can be calculated as follows

$$\Delta = \frac{1}{2}\int_0^L \left[\left(\frac{\partial u(z,t)}{\partial z} \right)^2 + \left(\frac{\partial v(z,t)}{\partial z} \right)^2 + (x^2 + y^2)\left(\frac{\partial \varphi(z,t)}{\partial z} \right)^2 - 2y\left(\frac{\partial u(z,t)}{\partial z} \right)\left(\frac{\partial \varphi(z,t)}{\partial z} \right) + 2x\left(\frac{\partial v(z,t)}{\partial z} \right)\left(\frac{\partial \varphi(z,t)}{\partial z} \right) \right] dz \tag{10}$$

Substituting Eqs. (7) and (10) into Eq. (9), the external potential energy obtained as follows

$$V_{ext} = \frac{1}{2}\int_0^L \left\{ P\left[\left(\frac{\partial u(z,t)}{\partial z} \right)^2 + \left(\frac{\partial v(z,t)}{\partial z} \right)^2 + r_m^2 \left(\frac{\partial \varphi(z,t)}{\partial z} \right)^2 - 2y_c \left(\frac{\partial u(z,t)}{\partial z} \right)\left(\frac{\partial \varphi(z,t)}{\partial z} \right) + 2x_c \left(\frac{\partial v(z,t)}{\partial z} \right)\left(\frac{\partial \varphi(z,t)}{\partial z} \right) \right] + \beta_1 M_r \left(\frac{\partial \varphi(z,t)}{\partial z} \right)^2 + 2M_r \left(\frac{\partial v(z,t)}{\partial z} \right)\left(\frac{\partial \varphi(z,t)}{\partial z} \right) + \beta_2 M_s \left(\frac{\partial \varphi(z,t)}{\partial z} \right)^2 - 2M_s \left(\frac{\partial u(z,t)}{\partial z} \right)\left(\frac{\partial \varphi(z,t)}{\partial z} \right) \right\} dz \tag{11}$$

which

$$\beta_1 = \frac{1}{I_r}\left[\int_A x^3 dA + \int_A xy^2 dA - x_G . r_G^2 A \right] \tag{12a}$$

$$\beta_2 = \frac{1}{I_s}\left[\int_A y^3 dA + \int_A yx^2 dA - y_G . r_G^2 A \right] \tag{12b}$$

The total potential energy of the beam can now be obtained by substituting Eqs. (6) and (11) in Eq. (5). Thus

$$V = \frac{1}{2}\int_0^L \left\{ \left[EI_x \left(\frac{\partial^2 u(z,t)}{\partial z^2} \right)^2 + EI_y \left(\frac{\partial^2 v(z,t)}{\partial z^2} \right)^2 + EI_w \left(\frac{\partial^2 \varphi(z,t)}{\partial z^2} \right)^2 + G_t J_t \left(\frac{\partial \varphi(z,t)}{\partial z} \right)^2 \right] - \left[P\left(\frac{\partial u(z,t)}{\partial z} \right)^2 + P\left(\frac{\partial v(z,t)}{\partial z} \right)^2 + \left(P.r_m^2 + \beta_1 M_r + \beta_2 M_s \right)\left(\frac{\partial \varphi(z,t)}{\partial z} \right)^2 + 2\left(M_r + Px_c \right)\left(\frac{\partial v(z,t)}{\partial z} \right)\left(\frac{\partial \varphi(z,t)}{\partial z} \right) - 2\left(M_s + Py_c \right)\left(\frac{\partial u(z,t)}{\partial z} \right)\left(\frac{\partial \varphi(z,t)}{\partial z} \right) \right] \right\} dz \tag{13}$$

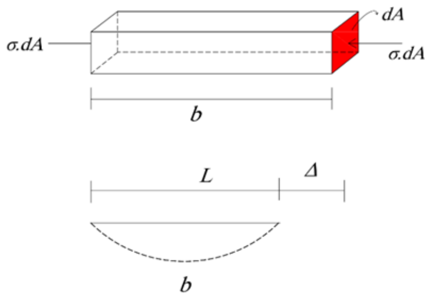

Fig. 2 (a) Longitudinal fiber (b) Difference in length between arc and chord

Eqs. (4) and (13) are now substituted into Eq. (2) and integrated. The derived governing differential equations for the considered beam element are as follows

$$EI_x\left(\frac{\partial^4 u(z,t)}{\partial z^4}\right)+P\left(\frac{\partial^2 u(z,t)}{\partial z^2}-y_c\frac{\partial^2 \varphi(z,t)}{\partial z^2}\right) -M_s\left(\frac{\partial^2 \varphi(z,t)}{\partial z^2}\right)-my_c\left(\frac{\partial^2 \varphi(z,t)}{\partial t^2}\right)+m\left(\frac{\partial^2 u(z,t)}{\partial t^2}\right)=0 \tag{14a}$$

$$EI_y\left(\frac{\partial^4 v(z,t)}{\partial z^4}\right)+P\left(\frac{\partial^2 v(z,t)}{\partial z^2}+x_c\frac{\partial^2 \varphi(z,t)}{\partial z^2}\right) +M_r\left(\frac{\partial^2 \varphi(z,t)}{\partial z^2}\right)+mx_c\left(\frac{\partial^2 \varphi(z,t)}{\partial t^2}\right) +m\left(\frac{\partial^2 v(z,t)}{\partial t^2}\right)=0 \tag{14b}$$

$$EI_w\left(\frac{\partial^4 \varphi(z,t)}{\partial z^4}\right)-G_tJ_t\left(\frac{\partial^2 \varphi(z,t)}{\partial z^2}\right) +P\left(r_m^2\left(\frac{\partial^2 \varphi(z,t)}{\partial z^2}\right)+x_c\left(\frac{\partial^2 v(z,t)}{\partial z^2}\right)-y_c\left(\frac{\partial^2 u(z,t)}{\partial z^2}\right)\right) +M_r\left(\frac{\partial^2 v(z,t)}{\partial z^2}\right)-M_s\left(\frac{\partial^2 u(z,t)}{\partial z^2}\right)+ (\beta_1 M_r+\beta_2 M_s)\left(\frac{\partial^2 \varphi(z,t)}{\partial z^2}\right)-my_c\left(\frac{\partial^2 u(z,t)}{\partial t^2}\right) +mx_c\left(\frac{\partial^2 v(z,t)}{\partial t^2}\right)+mr_m^2\left(\frac{\partial^2 \varphi(z,t)}{\partial t^2}\right)=0 \tag{14c}$$

The above equations are coupled and should be solved simultaneously. The associated boundary conditions at ends $(Z=0,L)$ are

$$\left[-EI_x\left(\frac{\partial^2 u(z,t)}{\partial z^2}\right)\right]\frac{\partial \delta u(z,t)}{\partial z}=0 \tag{15a}$$

$$\left[-EI_y\left(\frac{\partial^2 v(z,t)}{\partial z^2}\right)\right]\frac{\partial \delta v(z,t)}{\partial z}=0 \tag{15b}$$

$$\left[-EI_w\left(\frac{\partial^2 \varphi(z,t)}{\partial z^2}\right)\right]\frac{\partial \delta \varphi(z,t)}{\partial z}=0 \tag{15c}$$

$$\left[EI_x\left(\frac{\partial^3 u(z,t)}{\partial z^3}\right)-GA_x\left(\frac{\partial u(z,t)}{\partial z}-y_s\frac{\partial \varphi(z,t)}{\partial z}\right)+ P\left(\frac{\partial u(z,t)}{\partial z}-y_G\frac{\partial \varphi(z,t)}{\partial z}\right) -M_s\left(\frac{\partial \varphi(z,t)}{\partial z}\right)\right]\delta u(z,t)=0 \tag{15d}$$

$$\left[EI_y\left(\frac{\partial^3 v(z,t)}{\partial z^3}\right)-GA_y\left(\frac{\partial v(z,t)}{\partial z}+x_s\frac{\partial \varphi(z,t)}{\partial z}\right) +P\left(\frac{\partial v(z,t)}{\partial z}+x_G\frac{\partial \varphi(z,t)}{\partial z}\right)+M_r\left(\frac{\partial \varphi(z,t)}{\partial z}\right)\right]\delta v(z,t)=0 \tag{15e}$$

$$\left[EI_w\left(\frac{\partial^3 \varphi(z,t)}{\partial z^3}\right)+(\beta_1 M_r+\beta_2 M_s+r_G^2 P -GJ_o)\left(\frac{\partial \varphi(z,t)}{\partial z}\right)-(M_s+Py_G-GA_x y_s)\left(\frac{\partial u(z,t)}{\partial z}\right) +(M_r+Px_G-GA_y x_s)\left(\frac{\partial v(z,t)}{\partial z}\right)\right]\delta \varphi(z,t)=0 \tag{15f}$$

2.2 Dynamic stiffness matrix

The usual steps of assuming harmonic variation ($u(z,t)=U(z)e^{i\omega t}$, $v(z,t)=V(z)e^{i\omega t}$, $\varphi(z,t)=\Phi(z)e^{i\omega t}$) and the introduction of the non-dimensional variable($\xi=\frac{z}{L}$) then yields the governing Eqs. (14a), (14b) and (14c) as the following

$$U''''(\xi)+\lambda_x^2 U''(\xi)-(\lambda_x^2 y_c+\eta_x^2)\Phi''(\xi) -\beta_x^2\omega^2 U(\xi)+\beta_x^2 y_c\omega^2\Phi(\xi)=0 \tag{16a}$$

$$V''''(\xi)+(\lambda_y^2)V''(\xi)+(\lambda_y^2 x_c+\eta_y^2)\Phi''(\xi) -\beta_y^2\omega^2 V(\xi)-\beta_y^2 x_c\omega^2\Phi(\xi)=0 \tag{16b}$$

$$\Phi''''(\xi)+(\lambda_\varphi^2-\alpha_\varphi^2+\eta_{\varphi 1}^2+\eta_{\varphi 2}^2)\Phi''(\xi) -\left(\frac{1}{\gamma_x^2}\right)(\lambda_x^2 y_c+\eta_x^2)U''(\xi)+ \left(\frac{1}{\gamma_y^2}\right)(\lambda_y^2 x_c+\eta_y^2)V''(\xi)+\frac{\beta_x^2}{\gamma_x^2}\omega^2 y_c U(\xi) -\frac{\beta_y^2}{\gamma_y^2}\omega^2 x_c V(\xi)-\beta_\varphi^2\omega^2\Phi(\xi)=0 \tag{16c}$$

where

$$\beta_x^2=\frac{mL^4}{EI_x}\ ,\ \beta_y^2=\frac{mL^4}{EI_y}\ ,\ \beta_\varphi^2=\frac{mL^4}{EI_w}r_m^2 \quad \text{(17a-c)}$$

$$\eta_{\varphi 1}^2=\frac{\beta_1 M_r L^2}{EI_w}\ ,\ \eta_x^2=\frac{M_s L^2}{EI_x}\ ,\ \eta_y^2=\frac{M_r L^2}{EI_y} \quad \text{(17d-f)}$$

$$\lambda_x^2=\frac{PL^2}{EI_x}\ ,\ \lambda_y^2=\frac{PL^2}{EI_y}\ ,\ \lambda_\varphi^2=\frac{PL^2}{EI_w}r_m^2 \quad \text{(17g-i)}$$

$$\gamma_x^2=\frac{EI_w}{EI_x},\ \ \gamma_y^2=\frac{EI_w}{EI_y}\ ,\ \alpha_\varphi^2=\frac{G_t J_t L^2}{EI_w}\ ,\ \eta_{\varphi 2}^2=\frac{\beta_2 M_s L^2}{EI_w} \quad \text{(17j-m)}$$

U, V and Φ are the amplitudes of u, v and φ, respectively, and ω is the circular frequency.

Eq. (16) can be re-written in the following matrix form

$$\begin{bmatrix} D^4+\lambda_x^2D^2-\beta_x^2\omega^2 & 0 & -(\lambda_x^2 y_c+\eta_x^2)D^2+\beta_x^2 y_c\omega^2 \\ 0 & D^4+\lambda_y^2D^2-\beta_y^2\omega^2 & (\lambda_y^2 x_c+\eta_y^2)D^2-\beta_y^2 x_c\omega^2 \\ -(\frac{1}{\gamma_x^2})\left[(\lambda_x^2 y_c+\eta_x^2)D^2-\beta_x^2\omega^2 y_c\right] & (\frac{1}{\gamma_y^2})\left[(\lambda_y^2 x_c+\eta_y^2)D^2-\beta_y^2\omega^2 x_c\right] & D^4+(\lambda_\varphi^2-\alpha_\varphi^2+\eta_{\varphi 1}^2+\eta_{\varphi 2}^2)D^2-\beta_\varphi^2\omega^2 \end{bmatrix}\begin{bmatrix} U(\xi) \\ V(\xi) \\ \Phi(\xi) \end{bmatrix}=0 \quad (18)$$

in which $D=\dfrac{d}{d\xi}$.

Eq. (18) can be combined into one equation by eliminating all but one of U, V or Φ, to give the twelfth-order differential equation

$$(\mu_1 D^{12}+\mu_2 D^{10}+\mu_3 D^8+\mu_4 D^6+\mu_5 D^4 +\mu_6 D^2+\mu_7)W(\xi)=0 \quad (19)$$

where $W(\xi)=U(\xi), V(\xi)$ or $\Phi(\xi)$.

Lengthy expressions for the coefficients μ_i ,which could be obtained using MATLAB via symbolic computation, are not given here due to space limitations.

Eq. (19) is a linear differential equation with constant coefficients and hence solutions can be assumed in the form

$$W(\xi)=e^{a\xi} \quad (20)$$

Substituting Eq. (20) into Eq. (19) gives the auxiliary equation as

$$\mu_1\tau^6+\mu_2\tau^5+\mu_3\tau^4+\mu_4\tau^3+\mu_5\tau^2+ \mu_6\tau+\mu_7=0 \quad (21)$$

where $\tau=a^2$.

The solutions of Eq. (21) cannot be achieved in closed-form, therefore a numerical approach is necessary. Let the six-roots of Eq. (21) be τ_j (j=1,6) where these roots may be real or complex. Therefore the twelve roots of Eq. (19) can be obtained as

$$a_{2j-1}=\sqrt{\tau_j}\quad ,\ a_{2j}=-\sqrt{\tau_j}\quad (j=1{,}6) \quad (22)$$

The general solution to Eq. (19) is given by the following

$$W(\xi)=\sum_{j=1}^{12}C_j.e^{a_j\xi} \quad (23)$$

Eq. (23) represents the solution for $U(\xi)$, $V(\xi)$ and $\Phi(\xi)$, since they are related via Eq. (18). Hence, they can be written individually as follows

$$U(\xi)=\sum_{j=1}^{12}C_j^u.e^{a_j\xi}\quad V(\xi)=\sum_{j=1}^{12}C_j^v.e^{a_j\xi}$$
$$\Phi(\xi)=\sum_{j=1}^{12}C_j.e^{a_j\xi} \quad \text{(24a-c)}$$

The relationship between the constants C_j^u, C_j^v and C_j (j=1,6) also follows from Eq. (18) as follows

$$C_j^u=t_j^uC_j\quad ,C_j^v=t_j^vC_j\quad (j=1{,}12) \quad (25)$$

where

$$t_j^u=\frac{(\lambda_x^2 y_c+\eta_x^2)a_j^2-\beta_x^2 y_c\omega^2}{a_j^4+\lambda_x^2a_j^2-\beta_x^2\omega^2}$$
$$t_j^v=\frac{(-\lambda_y^2 x_c-\eta_y^2)a_j^2+\beta_y^2 x_c\omega^2}{a_j^4+\lambda_y^2a_j^2-\beta_y^2\omega^2} \quad \text{(26a,b)}$$
$$(j=1{,}12)$$

The expressions for shear forces $Q_x(\xi)$ and $Q_y(\xi)$, bending moments $M_x(\xi)$ and $M_y(\xi)$, torsional moment $T(\xi)$ and bi-moment $B(\xi)$ can be obtained from Eq. (15) as follows

$$M_x(\xi)=-A_xU''(\xi) \quad \text{(27a)}$$

$$M_y(\xi)=-A_yV''(\xi) \quad \text{(27b)}$$

$$B(\xi)=-D_o\Phi''(\xi) \quad \text{(27c)}$$

$$Q_x(\xi)=B_xU'''(\xi)+\rho\big(U'(\xi)-y_c\Phi'(\xi)\big)-H_1\Phi'(\xi) \quad \text{(27d)}$$

$$Q_y(\xi)=B_yV'''(\xi)+\rho\big(V'(\xi)+x_c\Phi'(\xi)\big)+G_1\Phi'(\xi) \quad \text{(27e)}$$

where

$$T(\xi)=E_o\Phi'''(\xi)+(G_2+H_2+\rho.r_m^2-F_o)\Phi'(\xi) -(H_1+\rho y_c)U'(\xi)+(G_1+\rho x_c)V'(\xi) \quad \text{(27f)}$$

$$A_x=\frac{EI_x}{L^2}\ ,\ A_y=\frac{EI_y}{L^2}\ ,\ B_x=\frac{EI_x}{L^3} \quad \text{(28a-c)}$$

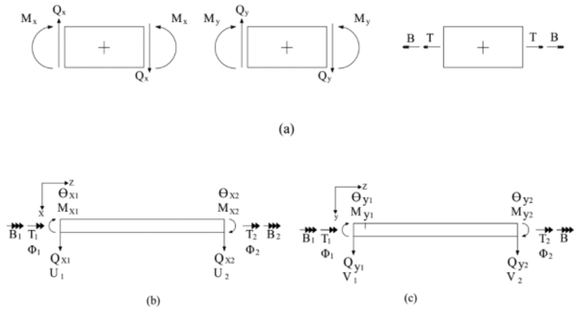

Fig. 3 (a) Sign convention for positive forces; (b) and (c) Sign convention for nodal displacements and forces

$$B_y = \frac{EI_y}{L^3} \quad , \quad \rho = \frac{P}{L} \quad , \quad D_o = \frac{EI_w}{L^2} \tag{28d-f}$$

$$E_o = \frac{EI_w}{L^3} \quad , \quad F_o = \frac{G_t J_t}{L} \quad , \quad G_1 = \frac{M_r}{L} \tag{28g-i}$$

$$G_2 = \frac{M_r B_1}{L} \quad , \quad H_1 = \frac{M_s}{L} \quad , \quad H_2 = \frac{M_s B_2}{L} \tag{28j-l}$$

From Fig. 3 the boundary conditions for the nodal displacements and forces are, respectively, the following

$$\xi = 0: \; U = U_1, \quad V = V_1, \quad \Phi = \Phi_1, \quad \Theta_x = \Theta_{x1}, \quad \Theta_y = \Theta_{y1}, \quad \Phi' = \Phi'_1 \tag{29a}$$

$$\xi = 1: \; U = U_2, \quad V = V_2, \quad \Phi = \Phi_2, \quad \Theta_x = \Theta_{x2}, \quad \Theta_y = \Theta_{y2}, \quad \Phi' = \Phi'_2 \tag{29b}$$

$$\xi = 0: \quad Q_x = Q_{x1}, \; Q_y = Q_{y1}, \; T = T_1, \quad M_x = M_{x1}, \; M_y = M_{y1}, \; B = B_1 \tag{29c}$$

$$\xi = 1: \; Q_x = -Q_{x2}, \; Q_y = -Q_{y2}, \quad T = -T_2, \quad M_x = -M_{x2}, \; M_y = -M_{y2}, \; B = -B_2 \tag{29d}$$

Θ_x and Θ_y are the amplitudes of $\theta_x(z,t)$ and $\theta_x(z,t)$, respectively (where $\theta_x(z,t)$ and $\theta_y(z,t)$ are the rotation of the cross-section due to bending in the $x-z$ and $y-z$ planes, respectively).

The nodal displacements can be determined from Eqs. (24) and (29a,b) and written in matrix form as follows

$$\boldsymbol{D} = \boldsymbol{BC} \tag{30}$$

where $\boldsymbol{D}$ is the nodal displacement vector, $\boldsymbol{C}$ is the vector of unknown constants and $\boldsymbol{B}$ is a coefficient matrix. They are defined as follows

$$\mathrm{D} = \{U_1 \quad V_1 \quad \Phi_1 \quad \Theta_{x1} \quad \Theta_{y1} \quad \Phi'_1 \quad U_2 \quad V_2 \quad \Phi_2 \quad \Theta_{x2} \quad \Theta_{y2} \quad \Phi'_2\}^T \tag{31a}$$

$$\mathrm{C} = \{C_1 \quad C_2 \quad C_3 \quad C_4 \quad C_5 \quad C_6 \quad C_7 \quad C_8 \quad C_9 \quad C_{10} \quad C_{11} \quad C_{12}\}^T \tag{31b}$$

$$\mathrm{B} = \begin{bmatrix} b_{1,1} & b_{1,2} & \cdots & b_{1,11} & b_{1,12} \\ b_{2,1} & b_{2,2} & \cdots & b_{2,11} & b_{2,12} \\ \vdots & \vdots & \ddots & \vdots & \vdots \\ b_{11,1} & b_{11,2} & \cdots & b_{11,11} & b_{11,12} \\ b_{12,1} & b_{12,2} & \cdots & b_{12,11} & b_{12,12} \end{bmatrix} \tag{32}$$

$$b_{1,j} = t_j^u \quad , \quad b_{2,j} = t_j^v \quad , \quad b_{3,j} = 1 \tag{33a-c}$$

$$b_{4,j} = \frac{a_j}{L} t_j^u \quad , \quad b_{5,j} = \frac{a_j}{L} t_j^v \quad , \quad b_{6,j} = \frac{a_j}{L} \tag{33d-f}$$

$$b_{7,j} = t_j^u e^{a_j} \quad , \quad b_{8,j} = t_j^v e^{a_j} \quad , \quad b_{9,j} = e^{a_j} \tag{33g-i}$$

$$b_{10,j} = \frac{a_j}{L} t_j^u e^{a_j} \; , \; b_{11,j} = \frac{a_j}{L} t_j^v e^{a_j} \; , \; b_{12,j} = \frac{a_j}{L} e^{a_j} \tag{33j-l}$$

where $(j = 1, 12)$.

Hence, the vector of constants $\mathbf{C}$ can be determined from Eq. (30) as the following

$$\mathbf{C} = \mathbf{B}^{-1}\mathbf{D} \tag{34}$$

In similar fashion, the vector of nodal forces can be determined from Eqs. (27) and (29c, d) as the following

$$\mathbf{F} = \mathbf{SC} \tag{35}$$

where $\mathbf{F}$ is the nodal force vector and $\mathbf{S}$ is a coefficient matrix. They are defined as follows

$$\mathrm{F} = \{Q_{x1} \quad Q_{y1} \quad T_1 \quad M_{x1} \quad M_{y1} \quad B_1 \quad Q_{x2} \quad Q_{y2} \quad T_2 \quad M_{x2} \quad M_{y2} \quad B_2\}^T \tag{36}$$

$$\mathrm{S} = \begin{bmatrix} s_{1,1} & s_{1,2} & \cdots & s_{1,11} & s_{1,12} \\ s_{2,1} & s_{2,2} & \cdots & s_{2,11} & s_{2,12} \\ \vdots & \vdots & \ddots & \vdots & \vdots \\ s_{11,1} & s_{11,2} & \cdots & s_{11,11} & s_{11,12} \\ s_{12,1} & s_{12,2} & \cdots & s_{12,11} & s_{12,12} \end{bmatrix} \tag{37}$$

in which

$$s_{1,j} = B_x t_j^u a_j^3 + (\rho) t_j^u a_j + (-\rho . y_c - H_1) a_j \tag{38a}$$

$$s_{2,j} = B_y t_j^v a_j^3 + (\rho) t_j^v a_j + (\rho . x_c + G_1) a_j \tag{38b}$$

$$s_{3,j}=E_o a_j^3+(G_2+H_2+\rho r_m^2-F_o)a_j -(H_1+\rho y_c)t_j^u a_j+(G_1+\rho x_c)t_j^v a_j \tag{38c}$$

$$s_{4,j}=-A_x.t_j^u a_j^2 \tag{38d}$$

$$s_{5,j}=-A_y.t_j^v a_j^2 \tag{38e}$$

$$s_{6,j}=-D_o a_j^2 \tag{38f}$$

$$s_{7,j}=-e^{a_j}[B_x t_j^u a_j^3+(\rho)t_j^u a_j+(-\rho.y_c-H_1)a_j] \tag{38g}$$

$$s_{8,j}=-e^{a_j}[B_y t_j^v a_j^3+(\rho)t_j^v a_j+(\rho.x_c+G_1)a_j] \tag{38h}$$

$$s_{9,j}=-e^{a_j}[E_o a_j^3+(G_2+H_2+\rho r_m^2-F_o)a_j -(H_1+\rho y_c)t_j^u a_j+(G_1+\rho x_c)t_j^v a_j] \tag{38i}$$

$$s_{10,j}=e^{a_j}A_x.t_j^u a_j^2 \tag{38j}$$

$$s_{11,j}=e^{a_j}A_y.t_j^v a_j^2 \tag{38k}$$

$$s_{12,j}=e^{a_j}D_o a_j^2 \tag{38l}$$

where $(j=1,12)$.

Thus the required stiffness matrix can be developed by substituting Eq. (34) into Eq. (35) to give

$$\boldsymbol{F}=\boldsymbol{KD} \tag{39}$$

where the exact dynamic stiffness matrix, $\mathbf{K}=\mathbf{SB^{-1}}$.

The dynamic stiffness matrix can now be used to compute the coupled bending-torsional natural frequencies of either a single eccentrically loaded Bernoulli-Euler thin-walled beam or an assembly of them. An accurate and reliable method of calculating the natural frequencies is to use the dynamic stiffness matrix in conjunction with the well-known Wittrick-Williams algorithm (1971).

2.3 Application of Wittrick-Williams algorithm

The Wittrick-Williams algorithm (1971) is widely understood and has been implemented in many different ways. Very often, it is possible to establish the clamped-clamped frequencies of a component member by examining the determinant of a coefficient matrix corresponding to $\mathbf{B}$ in Eq. (30) when $\mathbf{D}=\mathbf{0}$. However, this was not possible in the current case, since the elements of $\mathbf{B}$ could be complex. Instead, recourse was made to a procedure originally proposed by Howson and Williams (1973).

The reference shows that the key to converging on the required system frequencies lies in the calculation of two parameters, K_{ss} and J_{ss}, for each member of the structure in turn. K_{ss} is the dynamic stiffness matrix of a component member when the member is removed from the structure and then simply supported, while J_{ss} is the number of natural frequencies of this simply supported member that have been exceeded by the trial frequency. Simply supported boundary conditions for the beam member described herein are defined as follows

$$\xi=0 \text{ and } \xi=1: \quad M_x=M_y=B=0, \quad U=V=\Phi=0 \tag{40}$$

The stiffness relationship for a single member subject to these boundary conditions can then be obtained by deleting appropriate rows and columns from Eq. (39) to leave the following

$$\begin{bmatrix} M_{x1}\\ M_{y1}\\ B_1\\ M_{x2}\\ M_{y2}\\ B_2 \end{bmatrix}=\begin{bmatrix} k_{4,4} & k_{4,5} & k_{4,6} & k_{4,10} & k_{4,11} & k_{4,12}\\ k_{5,4} & k_{5,5} & k_{5,6} & k_{5,10} & k_{5,11} & k_{5,12}\\ k_{6,4} & k_{6,5} & k_{6,6} & k_{6,10} & k_{6,11} & k_{6,12}\\ k_{10,4} & k_{10,5} & k_{10,6} & k_{10,10} & k_{10,11} & k_{10,12}\\ k_{11,4} & k_{11,5} & k_{11,6} & k_{11,10} & k_{11,11} & k_{11,12}\\ k_{12,4} & k_{12,5} & k_{12,6} & k_{12,10} & k_{12,11} & k_{12,12} \end{bmatrix}\begin{bmatrix} \Theta_{1x}\\ \Theta_{1y}\\ \Phi_1'\\ \Theta_{2x}\\ \Theta_{2y}\\ \Phi_2' \end{bmatrix} \tag{41}$$

or

$$\mathbf{F}=\mathbf{K_{ss}d_{ss}} \tag{42}$$

where the $K_{i,j}$ are the remaining elements of $\mathbf{K}$ with their original row i and column j subscripts and K_{ss} is the required 6×6 matrix for this simple one member structure.

Application of the Wittrick-Williams algorithm (1971) to this simple structure gives the following

$$J_{ss}(\omega^*)=J_m(\omega^*)+s\{\mathrm{K}_{ss}(\omega^*)\} \tag{43}$$

$$J_m(\omega^*)=J_{ss}(\omega^*)-s\{\mathrm{K}_{ss}(\omega^*)\} \tag{44}$$

where $J_{SS}(\omega^*)$ is the number of natural frequencies of the simply supported member that lie below the trial frequency ω^*, $J_m(\omega^*)$ is the required number of clamped-clamped natural frequencies of the member lying below ω^* and $s\{K_{SS}(\omega^*)\}$ is the sign count of the matrix $K_{SS}(\omega^*)$. The evaluation of $s\{K_{SS}(\omega^*)\}$ is clearly straightforward, and the problem thus lies in determining $J_{SS}(\omega^*)$.

Based on Eqs. (24a, b and c) and (27a, b and c), the boundary conditions of Eq. (40) are satisfied by assuming solutions for the displacements $U(\xi)$, $V(\xi)$ and $\Phi(\xi)$ of the following form

$$U(\xi)=F_n\sin(n\pi\xi),\ V(\xi)=G_n\sin(n\pi\xi),\ \Phi(\xi)=H_n\sin(n\pi\xi) \tag{45}$$

where F_n, G_n and H_n are constants.

Substituting Eq. (45) into Eq. (18) gives the following

$$\mathbf{AE=0} \tag{46}$$

where

$$\mathrm{E} = \begin{bmatrix} F_n \\ G_n \\ H_n \end{bmatrix} \tag{47a}$$

$$\mathrm{A} = \begin{bmatrix} (n\pi)^4 - \lambda_x^2 (n\pi)^2 - \beta_x^2 \omega^2 & \mathbf{0} & (\lambda_x^2 y_c + \eta_x^2)(n\pi)^2 + \beta_x^2 y_c \omega^2 \\ 0 & (n\pi)^4 - \lambda_y^2 (n\pi)^2 - \beta_y^2 \omega^2 & -(\lambda_y^2 x_c + \eta_y^2)(n\pi)^2 - \beta_y^2 x_c \omega^2 \\ (\frac{1}{\gamma_x^2})\left[(\lambda_x^2 y_c + \eta_x^2)(n\pi)^2 + \beta_x^2 \omega^2 y_c\right] & (\frac{1}{\gamma_y^2})\left[-(\lambda_y^2 x_c + \eta_y^2)(n\pi)^2 - \beta_y^2 \omega^2 x_c\right] & (n\pi)^4 + (\lambda_\varphi^2 - \alpha_\varphi^2 + \eta_{\varphi 1}^2 + \eta_{\varphi 2}^2)(n\pi)^2 - \beta_\varphi^2 \omega^2 \end{bmatrix} \tag{47b}$$

ω represents the coupled natural frequencies of the member with simply supported ends. The non-trivial solution of Eq. (46) is obtained when

$$|\mathbf{A}| = 0 \tag{48}$$

Eq. (48) can be expressed as a sixth-order polynomial equation in ω, and consequently, its real positive roots are the natural frequencies for each value of n=1, 2, 3… It is then possible to calculate $J_{ss}(\omega^*)$ by substituting progressively larger values of n until all of those natural frequencies lying below ω^* have been accounted for. Once $J_{ss}(\omega^*)$ is known, $J_m(\omega^*)$ can be calculated from Eq. (44).

3. Numerical results

Example I: In this example a cantilever steel beam with channel section (mono-symmetric section) is considered (Fig. 4). Characteristics of the desired section is given below:

$E = 2.164\times10^{11} Nm^2$, $I_y = 0.45\times10^{-6} m^4$

$I_x = 0.47348\times10^{-6} m^4$, $I_w = 0.1636\times10^{-9} m^6$

$G_t J_t = 11.21 N.m^2$, $r_m = 0.058827m$

$x_c = 0.03771m$, $y_c = 0.0m$

$m = 2.095(kg/m)$, $L = 1.28m$

$\beta_1 = 0.123519m$, $\beta_2 = 0.0m$, $h = 0.1m$

$b = 0.058m$, $t_f = 0.00125m$, $t_w = 0.00125m$

In Table 1, the first four natural frequencies of the beam obtained using proposed method are compared with results of finite element ABAQUS software. 700 ABAQUS's eight-noded shell element (S8R5) is used for modeling thin-walled beam in ABAQUS software.

The effect of increase of axial load and the effect of various eccentricities of axial load on natural frequencies of the channel beam are investigated in this example. The first three mode shapes of the unloaded channel beam (i.e., P = 0) are shown in Fig. 5. Note that in this figure the Φ component of the mode shapes have been multiplied by the distance x_c in order to compare Φ directly with the V component. According to Fig. 5 can be seen that the first and third mode shapes are coupled bending-torsional modes but the second mode shape is an uncoupled bending mode.

In first step of parametric study, the effect of increase of central axial load ($e_r = 0$, $e_s = 0$) on first three natural frequencies are investigated and are shown in Fig. 6. It should be noted that the beam is loaded in the range of zero to critical buckling load ($P_{cr} = 17653.214N$). According to Fig. 6. can be seen that natural frequencies are reduced by increasing the axial load. It should be noted that with the increasing frequency order, the effect of axial force on natural frequencies quickly reduces.

In second step of the parametric study, the effect of various eccentricities of axial load on natural frequencies of the channel beam are investigated. This step consists of two stage:

1- The effect of increasing of e_r (eccentricity along the axis of symmetry ($e_s = 0$)) on natural frequencies;

2- The effect of increasing of e_s (eccentricity along the axis perpendicular to the axis of symmetry ($e_r = 0$)) on natural frequencies.

In Table 2, the maximum possible values of e_r and e_s are given for different axial loads. Eccentricities e_r and e_s are chosen so that for selected eccentricities, considered axial load is the critical load (buckling load of first buckling mode).

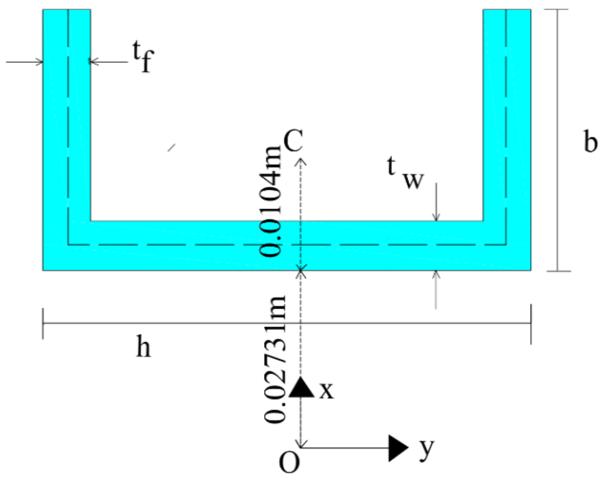

Fig. 4 Mono-symmetric channel section

Table 1 Natural frequencies (Hz) for the cantilever channel beam studied in Example I

Frequency number	$P = 0$		Centric axial load $P = 2500N$	
	Proposed method	ABAQUS	Proposed method	ABAQUS
1	25.3702	25.097	24.1093	24.029
2	75.5333	75.124	74.7521	74.332
3	98.5570	95.974	97.3494	95.084
4	148.6504	148.30	146.8254	147.320

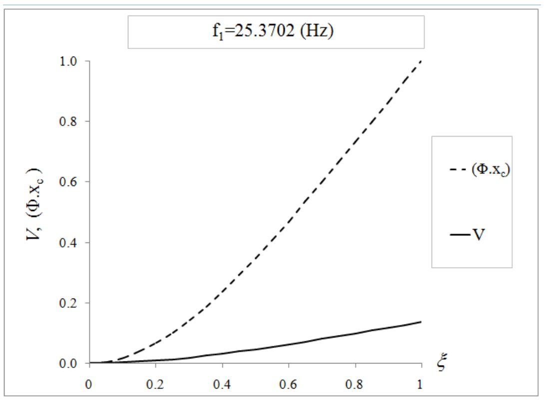

(a) First mode shape

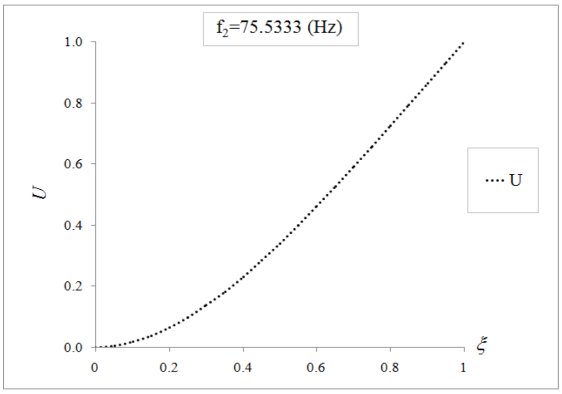

(b) Second mode shape

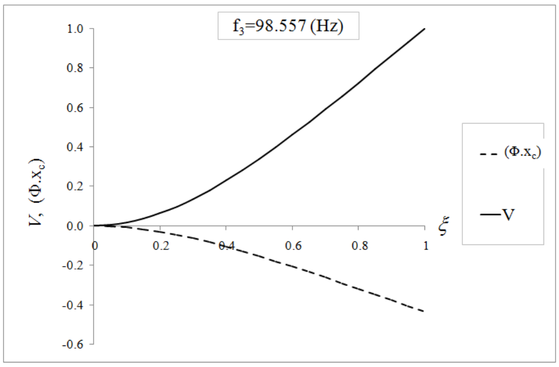

(c) Third mode shape

Fig. 5 Mode shapes of channel beam

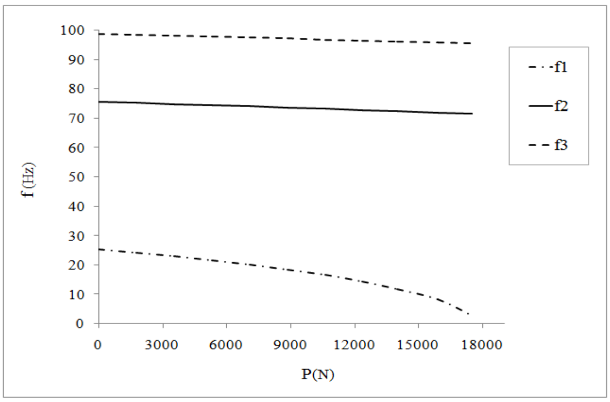

Fig. 6 The effect of increase of central axial load on natural frequencies of channel beam

Table 2 Possible values of e_r and e_s for different axial loads

$P(N)$	$0.2P_{cr}$	$0.4P_{cr}$	$0.6P_{cr}$
	3530.643	7061.286	10591.930
		e_s=0	
e_r (m)	0.115271	0.043278	0.019258
(e_r/b)	1.98743	0.74617	0.33204
		e_r=0	
e_s (m)	0.794473	0.341887	0.184936
(e_s/h)	7.94473	3.41887	1.849359

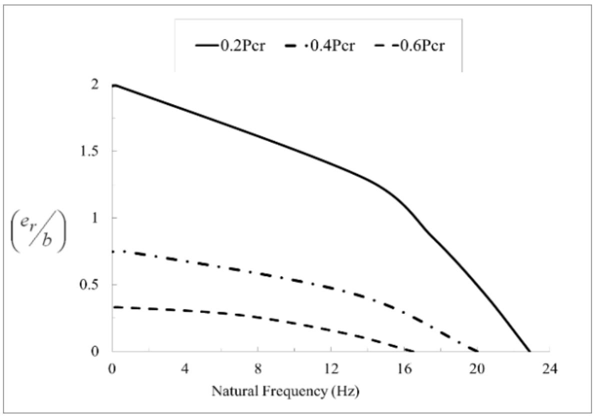

(a) First mode

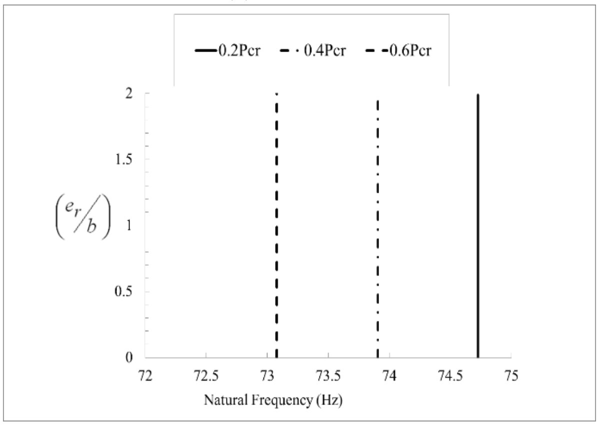

(b) Second mode

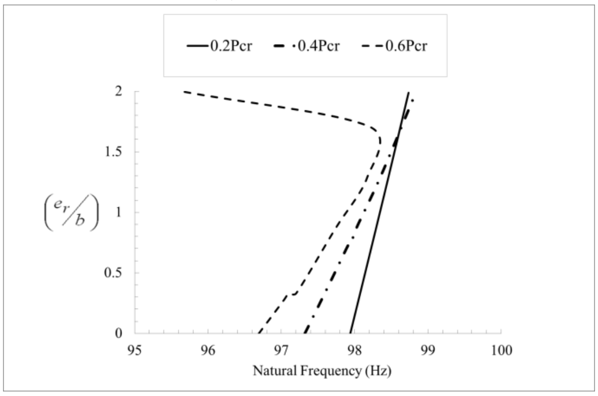

(c) Third mode

Fig. 7 Effect of increasing of e_r on natural frequencies of channel beam for different value of axial loads

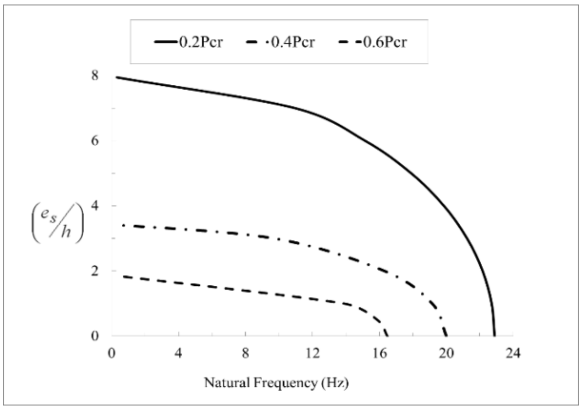

(a) First mode

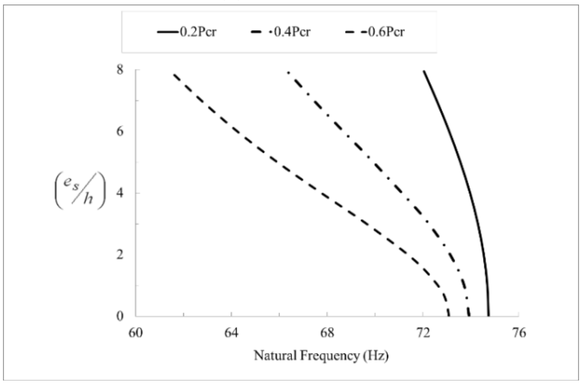

(b) Second mode

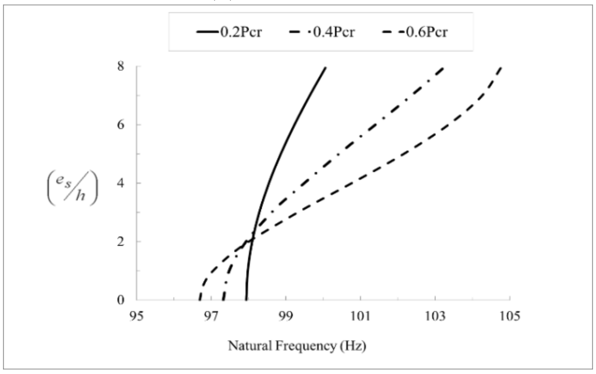

(c) Third mode

Fig. 8 Effect of increasing of e_s on natural frequencies of channel beam for different value of axial loads

In Figs. 7-8 effect of increasing of dimensionless parameters (e_r/b) and (e_s/h) on first three natural frequencies of beam, are given for different value of axial loads.

Considering Figs. 7-8, for a mono-symmetric section if eccentricity of axial load be along the axis of symmetry, increasing of eccentricity e_r will not affect the natural frequency of uncoupled bending mode along the axis of symmetry. However the natural frequency of coupled bending-torsional modes change during increasing e_r. If eccentricity of axial load be along the axis perpendicular to the axis of symmetry while increasing eccentricity e_s the natural frequency of uncoupled bending mode decreases. But the changes of natural frequency of coupled bending-torsional modes does not follow the certain relationship.

Table 3 Natural frequencies (Hz) for the asymmetric cantilever beam studied in Example II: (A) Proposed method (Axial load ignored); (B) Tanaka and Bercin (1999)(Axial load ignored); (C) Proposed method (Centric axial load P=2000N); (D) Shirmohammadzade *et al.* (2011) (Centric axial load P=2000N) (E) Proposed method (Eccentric axial load P=2000N (e_r=0.03 m, e_s=0.02 m))

Frequency number	Natural frequency (Hz)				
	(A)	(B)	(C)	(D)	(E)
1	17.1764	17.03	15.5625	15.5630	12.4103
2	27.3235	27.58	26.3266	26.3267	26.0903
3	59.1326	59.25	58.6767	58.6769	58.5448
4	98.7343	-	96.8216	96.8217	93.4513
5	167.4119	-	166.2883	166.2884	166.094

Example II: This example considers the beam studied by Tanaka and Bercin (1999). It is a uniform thin-walled beam of length 1.5 m with doubly asymmetric cross-section. The properties of the cross-section are as follows:

$EI_x = 73480\text{N.m}^2$, $EI_y = 16680\text{N.m}^2$

$EI_w = 26.34m^6$, $G_tJ_t = 10.81N.m^2$

$r_m = 0.055m$, $x_c = 0.02316m$

$y_c = 0.02625m$, $m = 1.947(kg/m)$

$L = 1.5m$, $\beta_1 = 0.045m$, $\beta_2 = 0.243m$

Table 3 shows the first five coupled natural frequencies of the beam for various cases. The results compared with results of Tanaka and Bercin (1999) and Shirmohammadzade *et al*. (2011).

3. Conclusions

A general formulation for free vibration analysis of three-dimensional non-symmetric axially loaded thin-walled Bernoulli-Euler beam considering the effects of eccentricity of axial load relative to centroid has been presented. The partial differential equations governing have been derived through application of Hamilton's principle. These equations are subsequently solved and presented in the form of a dynamic stiffness matrix. The application of such theory necessitates the solution of a transcendental eigenvalue problem. This has been accommodated in the present case by use of the Wittrick-Williams algorithm, which enables convergence upon any required frequency to any desired accuracy with the certain knowledge that none have been missed. The resulting matrix can be used to establish more complex beam systems and axially loaded tall building structures in usual way. Application of the dynamic stiffness matrix has been demonstrated by solving a parametric study numerical example in conjunction with the Wittrick-Williams algorithm.

References

Banerjee, J.R. (1989), "Coupled bending torsional dynamic stiffness matrix for beam elements", *Int. J. Numer. Method. Eng.*, **28**(6), 1283-1298.

Banerjee, J.R. (1991), "A Fortran routine for computation of coupled bending-torsional dynamic stiffness matrix of beam elements", *Adv. Eng. Softw.*, **13**(1), 17-24.

Banerjee, J.R. and Williams, F.W. (1992), "Coupled bending-torsional dynamic stiffness matrix for Timoshenko beam elements", *Comput. Struct.*, **42**(3), 301-310.

Banerjee, J.R. and Fisher, S.A. (1992), "Coupled bending-torsional dynamic stiffness matrix for axially loaded beam elements", *Int. J. Numer. Method. Eng.*, **33**(4), 739-751.

Banerjee, J.R. and Williams, F.W. (1994), "Coupled bending-torsional dynamic stiffness matrix for an axially loaded Timoshenko beam element", *Int. J. Solid. Struct.*, **31**(6), 749-762.

Banerjee, J.R., Guo, S. and Howson, W.P. (1996), "Exact dynamic stiffness matrix of a bending-torsion coupled beam including warping", *Comput. Struct.*, **59**(4), 613-621.

Banerjee, J.R. (1997), "Dynamic stiffness formulation for structural elements: A general approach", *Comput. Struct.*, **63**(1), 101-103.

Chen, C. H., Zhu, Y. F., Yao, Y. and Huang, Y. (2016), "The finite element model research of the pre-twisted thin-walled beam", *Struct. Eng. Mech.*, **57**(3), 389-402.

Chen, H.H. and Hsiao, K.M. (2007), "Coupled axial-torsional vibration of thin-walled Z-section beam induced by boundary conditions", *Thin-Wall. Struct.*, **45**(6), 573-583.

Eken, S. and Kaya, M.O. (2015), "Flexural-torsional coupled vibration of anisotropic thin-walled beams with biconvex cross-section", *Thin-Wall. Struct.*, **94**, 372-383.

Eslimy-Isfahany, SH.R. and Banerjee J.R. (1996), "Dynamic response of an axially loaded bending-torsion coupled beam", *J. Aircraft*, **33**(3), 601-607.

Eslimy-Isfahany, S.H.R., Banerjee, J.R. and Sobey, A.J. (1996), "Response of a bending-torsion coupled beam to deterministic and random loads", *J. Sound Vib.*, **195**, 267-283.

Ghandi, E., Rafezy, B. and Howson, W.P. (2012), "On the bi-planar motion of a Timoshenko beam with shear resistant in-fill", *Int. J. Mech. Sci.*, **57**(1), 1-8.

Ghandi, E., Rafezy, B., Abedi, K. and Howson, W.P. (2015), "Coupled flexural-torsional dynamic stiffness matrix of an elastically supported axially loaded beam with shear resistant in-fill", *Struct. Des. Tall Spec. Build.*, **24**(7), 537-554.

Howson, W.P. and Williams, F.W. (1973), "Natural frequencies of frames with axially loaded Timoshenko members", *J. Sound Vib.*, **26**(4), 503-515.

Jun, L., Rongying, S., Hongxing, H. and Xianding J. (2004) "Response of monosymmetric thin-walled Timoshenko beams to random excitations", *Int. J. Solid. Struct.*, **41**,6023-6040.

Kim, N.I. (2009), "Series solutions for spatially coupled buckling anlaysis of thin-walled Timoshenko curved beam on elastic foundation", *Struct. Eng. Mech.*, **33**(4), 447-484.

Rafezy, B. and Howson W.P. (2007), "Exact dynamic stiffness matrix for a thin-walled beam of doubly asymmetric cross-section filled with shear sensitive material", *Int. J. Numer. Method. Eng.*, **69**(13), 2758-2779.

Sheikh, A.H., Asadi, A. and Thomsen, O.T. (2015), "Vibration of thin-walled laminated composite beams having open and closed sections", *Compos. Struct.*, **134**, 209-215.

Shirmohammadzade, A., Rafezy, B. and Howson, W.P. (2011), "Exact dynamic stiffness matrix for a thin-walled beam-column of doubly asymmetric cross-section", *Struct. Eng. Mech.*, **38**(2),195-210.

Tanaka, M. and Bercin, A.N. (1999), "Free vibration solution for uniform beams of nonsymmetrical cross section using Mathematica", *Comput. Struct.*, **71**(1), 1-8.

Wittrick, W.H. and Williams, F.W. (1971), "A general algorithm for computing natural frequencies of elastic structures", *Quart. J. Mech. Appl. Math.*, **24**(3), 263-284.

CC